Surface Segregation in Supported Pd−Pt Nanoclusters and Alloys

L. C. A. van den Oetelaar, O. W. Nooij, S. Oerlemans, A. W. Denier van der Gon,* and H. H. Brongersma

Faculty of Physics and Schuit Institute of Catalysis, Eindhoven University of Technology, P.O. Box 513, 5600 MB Eindhoven, The Netherlands

L. Lefferts

DSM Research, P.O. Box 18, 6160 MD Geleen, The Netherlands

A. G. Roosenbrand

Shell Research and Technology Centre Thornton, P.O. Box 1, Chester CH1 3SH, England

J. A. R. van Veen

Shell Research and Technology Centre Amsterdam (SRTCA), Badhuisweg 3, 1031 CM Amsterdam, The Netherlands

Received: October 21, 1997; In Final Form: January 22, 1998

Surface segregation processes in Pd−Pt alloys and bimetallic Pd−Pt nanoclusters on alumina and carbon supports (technical catalysts) have been investigated by determining the metal surface composition of these systems by low-energy ion scattering (LEIS). Both Pd-rich ($Pd_{80}Pt_{20}$) and Pt-rich ($Pd_{20}Pt_{80}$) systems have been studied. The surface of the Pd−Pt alloys is enriched in Pd after heating in ultrahigh vacuum and thermodynamic equilibrium is reached at about 700 °C. Pd surface segregation is enhanced by heating the alloys in hydrogen or oxygen, and thermodynamic equilibrium is reached already at about 400−500 °C. For Pd−Pt catalysts with low metal dispersions of about 0.3 and 0.8, Pd surface segregation does take place during heating in hydrogen to approximately the same extent as in the Pd−Pt bulk alloys. For Pd−Pt catalysts with a high metal dispersion close to 1, however, surface segregation is completely suppressed during heating in hydrogen and oxygen. We attribute this to the limited supply of Pd atoms from the bulk to the surface of the nanoclusters.

1. Introduction

Small supported bimetallic clusters are important in heterogeneous catalysis.[1,2] From a technological point of view they are of interest in chemical processes such as catalytic reforming of petroleum naphtha fractions to produce high octane number components for gasolines. From a fundamental point of view they are of interest in elucidating the catalytic mechanism(s) on supported metal catalysts. In this case, also (single crystalline) alloys have been used to facilitate the study of the bimetallic surface chemistry.[3,4] The outermost atomic layer of the surface of these bimetallic clusters and alloys plays an important role in the catalytic process and the surface composition determines properties such as selectivity and lifetime of the catalyst.[1,2]

The surface composition of alloys, in particular the composition of the topmost surface layer, is generally different from the bulk composition due to segregation processes.[5−11] The equilibrium surface composition of bimetallic alloys is generally considered to be determined by the following parameters: the temperature, the metal surface free energies, the heat of mixing, the metal atomic sizes, and the presence of adsorbates. A prediction of the amount of surface enrichment of one of the constituents can be made using theoretical models that describe surface segregation (see, e.g., refs 7 and 12−16), such as the "broken bond" model. Complications in predicting the equilibrium surface composition arise when absorption-induced segregation,[17] surface segregation of bulk impurities,[18−20] a phase transition at the surface,[21] or sublimation of one of the constituents occurs.[18]

Additionally, in the case of supported bimetallic nanoclusters the cluster size and the interaction between the clusters and support are of importance. This may result in large differences in surface segregation between supported nanometer-sized clusters and bulk alloys, as was e.g. illustrated by Gijzeman using Monte Carlo simulations.[22] The cluster size may influence surface segregation by the limited supply of atoms and by the reduction in coordination number of the surface atoms.[12,22−25] The metal−support interaction may influence surface segregation by preferential anchoring of one of the constituents to the support at the cluster−support interface.[22,26−29] Since the influence of the cluster size and the metal−support interaction on the surface composition is largely unknown, detailed experimental studies of the outermost atomic layer of small supported bimetallic clusters are necessary.

Techniques such as extended X-ray absorption fine structure (EXAFS), X-ray photoelectron spectroscopy (XPS), Auger electron spectroscopy (AES), electron microscopy, IR spectroscopy, and chemisorption methods have been applied to characterize supported bimetallic clusters (see e.g., refs 30−33).

S1089-5647(97)03395-6 CCC: $15.00
Published on Web 04/09/1998

However, each technique has its limitations in probing the outermost atomic layer of the surface. Studies using EXAFS require complicated data analysis to extract the desired information and data interpretation may be ambiguous. Surface analysis techniques such as XPS and AES probe several nanometers deep. As shown by Sault,[34] it is not possible with these techniques to differentiate between homogeneous alloy clusters and clusters in which one component has segregated to the surface for cluster sizes smaller than approximately 6 nm. IR spectroscopy of species adsorbed on the supported clusters and chemisorption methods give only indirect information about the surface of clusters, and the surface may be modified by the adsorbates used.

Low-energy ion scattering (LEIS) is sensitive only to the topmost surface layer (see, e.g., ref 35) and is, therefore, very suitable to study surface segregation as has been shown for various bimetallic alloys (see, e.g., refs 36−40). However, one should be careful in performing ion-scattering experiments on small clusters because damage by sputtering does occur and the sputter yield of metal clusters may be significantly larger than that of bulk metal.[41] Sputtering may also change the surface composition by preferential sputtering and radiation-enhanced segregation and diffusion.[42−44] Therefore, static measurements (using a very low ion dose) are required. The metal loading of bimetallic catalysts is in general rather low (typically 1 wt % metal). The requirement of static analysis implies in this case also the requirement of a very sensitive analyzer.

In this paper, results are presented of static LEIS measurements of supported bimetallic Pd−Pt nanoclusters (technical catalysts) after treatments in hydrogen and oxygen at various temperatures in the range 25−500 °C. We will discuss the role of adsorbates/absorbates, cluster size, and metal−support interaction in the surface segregation process in supported nanoclusters in general and demonstrate the influence of these parameters on surface segregation in the Pd−Pt catalysts in particular. Bimetallic Pd−Pt catalysts are of great technological interest because they are applied in (de)hydrogenation reactions,[45−52] oxidation reactions,[53,54] (dehydro)cyclization reactions,[55−57] reduction of nitrate in the nylon production,[58] and the hydrogen peroxide production,[59,60] and the Pd−Pt system is also used in electrochemical studies.[61,62] The Pd−Pt system has the advantage that it is more resistant to poisoning by sulfur and nitrogen compounds than the respective monometallic catalysts.[46,63,64] We have also studied Pd−Pt bulk alloys with the same bulk composition as the nanoclusters to find out whether surface segregation in the nanoclusters is different from that in alloys. The surface composition of the Pd−Pt alloys has been determined with LEIS after treatments in UHV, hydrogen, and oxygen at various temperatures. The experimental results are compared with theoretical predictions of the equilibrium surface composition as a function of temperature. Both Pd- and Pt-rich samples have been studied. It will be shown that the surface composition of supported nanoclusters can be completely different from that of the bulk alloys after treatments in hydrogen and oxygen at elevated temperatures.

2. Experimental Section

2.1. Pd−Pt Catalysts and Bulk Alloys. Pd−Pt nanoclusters supported on γ-alumina or carbon (technical catalysts) and with different metal dispersions have been studied. Alumina supported Pd−Pt catalysts were prepared at the Shell Research and Technology Centre in Amsterdam (SRTCA) by impregnation of a γ-Al_2O_3 support (200 m^2/g) with Pd and Pt tetraamine complexes followed by calcination at 320 °C in air. It was found by dedicated scanning transmission electron microscopy measurements of similar Pd−Pt catalysts that bimetallic clusters are present.[65] The metal loadings used are 0.2 wt % Pd + 1.3 wt % Pt (atomic bulk composition of $Pd_{20}Pt_{80}$) and 0.7 wt % Pd + 0.3 wt % Pt (atomic bulk composition of $Pd_{80}Pt_{20}$). A carbon-supported Pd−Pt catalyst was obtained from DSM, with a metal loading of 6.0 wt % Pd + 4.0 wt % Pt (atomic bulk composition of $Pd_{73}Pt_{27}$).

To get information about the metal dispersion, chemisorption measurements have been performed. The metal dispersion of the $Pd_{20}Pt_{80}/Al_2O_3$ catalyst was determined by hydrogen chemisorption using the method of Kip et al.[66] A H/(Pd + Pt) ratio of 1.36 ± 0.1 was found, which indicates that the metal dispersion is close to 1 and that the average cluster diameter of this catalyst is 1 nm or smaller. The $Pd_{80}Pt_{20}/Al_2O_3$ catalyst is supposed to have a similar metal dispersion as the $Pd_{20}Pt_{80}/Al_2O_3$ catalyst. Electron microscopy measurements of the highly dispersed Pd−Pt catalysts have also been performed. Although some particles with a diameter of 2−7 nm were found, the major part of the metals is present as clusters smaller than about 1 nm, which is the detection limit of the electron microscope. To investigate the influence of the cluster size on surface segregation, an alumina-supported catalyst with a lower metal dispersion was studied. A $Pd_{80}Pt_{20}/Al_2O_3$ catalyst with a higher metal loading (2.26 wt % Pd + 1.03 wt % Pt) was prepared as described above and heated in hydrogen at 700 °C at the SRTCA before LEIS analysis. This catalyst has a metal dispersion of about 0.8, as indicated by electron microscopy and IR spectroscopy of adsorbed CO species. The metal dispersion of the carbon supported Pd−Pt catalyst is determined by the CO chemisorption method as described in ref 67. The metal surface area of the $Pd_{73}Pt_{27}$/C catalyst is found to be 89 m^2/g metal, when assuming a metal surface density of 1.45×10^{15} atoms/cm^2 and a CO/metal surface stochiometry of 1. Then the metal dispersion is approximately 0.3 and the average cluster diameter is about 5 nm. We note that this catalyst may have a rather broad cluster size distribution with clusters ranging from 2 to 10 nm in diameter; however, we believe that this does not significantly influence our interpretation of the LEIS measurements presented in this paper.

Prior to LEIS analysis, the catalyst pellets were powdered in a mortar and pressed with a load of 1600 kg/cm^2 in a tantalum cup. We suppose that this procedure does not influence the LEIS results significantly, since the sample preparation conditions are not critical to reproduce the LEIS measurements. Treatments with hydrogen and oxygen (500 mbar) at temperatures between 25 and 550 °C for 30 min (gas was refreshed after 15 min) were carried out in a preparation chamber connected to the ultrahigh-vacuum (UHV) chamber of the LEIS apparatus. The sample temperature in the preparation chamber was monitored by an in situ thermocouple. The maximum heating temperature in the pretreatment chamber is 550 °C, which limits the temperature treatments in a hydrogen or oxygen ambient.

Polycrystalline $Pd_{20}Pt_{80}$ and $Pd_{80}Pt_{20}$ bulk alloys were used as a reference and were chemically cleaned by etching in an acidic mixture of three parts of HCl (36% concentrated) and one part of HNO_3 (60% concentrated), followed by washing in ethanol and polishing with alumina powder. Sputtering with 3 keV Ne^+ (about 150 nA/cm^2) for 16 h at room temperature and at elevated temperature (800 °C) was done in the UHV chamber to remove any remaining contaminants on the alloys. (Due to

a different heating system, higher anneal temperatures can be applied in the UHV system than in the pretreatment chamber.) The absence of contaminants was checked by XPS and LEIS. The temperature of a sample in the UHV main chamber was monitored by a pyrometer. The accuracy of the sample temperature in the preparation chamber and UHV chamber was estimated to be ±25 °C, the reproducibility; however, was within 10 °C.

The surface composition of the Pd−Pt alloys has been studied by LEIS after heat treatments in the UHV chamber up to 800 °C and after treatments with hydrogen and oxygen (500 mbar) in the preparation chamber at temperatures between 25 and 550 °C for 30 min. Prior to LEIS analysis, the alloys were sputter cleaned at room temperature with 3 keV Ne^+ ions (about 150 nA/cm^2) for 16 h.

2.2. LEIS Analysis. The experiments have been carried out in the ERISS setup. It is equipped with an ion source (Leybold type IQE-12/38), a twin anode X-ray source (VG type 427) and an electrostatic energy analyzer. The primary ions are mass selected, focused, and directed perpendicular onto the target. Ions scattered over 145° are accepted by the analyzer. The analyzer is a double-toroidal electrostatic energy analyzer, similar to that of the EARISS setup, which has been described in more detail elsewhere.[68,69] Dependent on the polarity of the electrostatic deflection plates, it can analyze positive ions (for LEIS analysis) or electrons (for XPS analysis). This analyzer makes a very efficient use of the backscattered particles by measuring simultaneously a considerable part of the energy spectrum of the backscattered particles and 320° of the azimuthal spectrum. In addition, the sample manipulator can be scanned under the ion beam during measurements, effectively increasing the beam spot and thus reducing the necessary ion dose even more. To prevent charging of insulating materials, the surface of the sample is flooded from all azimuths with low-energy electrons. This UHV setup has a base pressure in the low 10^{-10} mbar range which increases to the $10^{-9}-10^{-8}$ mbar range during LEIS experiments due to the noble-gas influx.

The LEIS measurements are done with 3 keV Ne^+ ions at room temperature with an ion beam current of typically 1.0 nA and a 3 × 3 mm^2 spot size which results in an ion dose of typically 1.7 × 10^{13} ions/cm^2 per measurement. Under these conditions, the Ne^+ ions interact with about 1% of the total number of surface atoms per measurement and static measurements were obtained,[70] as shown by the negligible difference between two successive LEIS spectra from supported Pd−Pt nanoclusters treated with oxygen or hydrogen (see Figure 1).

In previous studies of Pd−Pt alloys[70,71] it was found that adsorption of hydrogen and oxygen on a metal surface results in a decrease of the metal LEIS signals with a factor of 10 or more with respect to the LEIS signals of the clean metal surfaces. However, no significant influence of hydrogen or oxygen was observed on the quantification of the surface composition of the Pd−Pt system, since the decrease of the LEIS signals was found to be independent of the constituent elements for this system.[70,71] Furthermore, upon sputtering of Pd−Pt alloys covered with hydrogen or oxygen, the ion beam induced desorption of the adsorbates was observed to be the same for Pd and Pt, as was already shown for desorption of oxygen on Pd and Pt substrates by Taglauer et al.[72]

The surface composition has been determined by calibration against polycrystalline reference samples,[73,74] assuming that matrix effects are absent. Because both the surface concentrations (about 1.6 × 10^{15} atoms/cm^2 for Pd and Pt) and the LEIS signals of the Pd and Pt references when using 3 keV Ne^+ ions

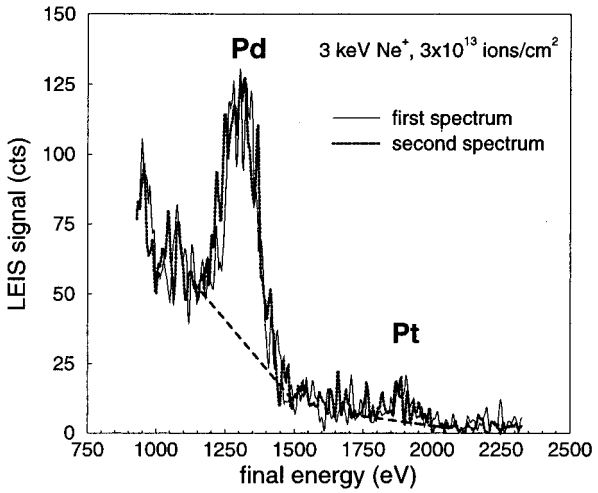

Figure 1. Static LEIS measurements of a $Pd_{80}Pt_{20}/Al_2O_3$ catalyst (3.3 wt % metal, metal dispersion of about 0.8) after treatment in 500 mbar of hydrogen at 400 °C. The long dashed curve illustrates the background subtraction method used for the integration of the peak areas.

are equal within experimental error, the atomic Pd surface fraction x_{Pd}^{surf} has been calculated by $S_{Pd}/(S_{Pd} + S_{Pt})$. The metal LEIS signal S_i has been obtained by taking the peak area of element i after linear background subtraction (as shown in Figure 1). It was found that the total metal signals of both alloys and references measured at a temperature of about 400 °C (to eliminate roughness effects) are equal within experimental error (±10%), which indicate that matrix effects are absent.[74] The good agreement between the experimental and theoretical sputter-equilibrium composition of both the alloys and clusters as presented in the next sections indicate that matrix effects are absent and that quantification by calibration can be done. This is also confirmed by previous work by Du Plessis et al., who used a similar quantification of ion-scattering spectra in a study of preferential sputtering and radiation enhanced segregation in Pt−Pd alloys.[75]

3. Results and Discussion of Surface Segregation in Pd−Pt Alloys

Before focusing on surface segregation in Pd−Pt nanoclusters, the results for the Pd−Pt alloys are presented and discussed in order to determine the influence of the temperature and the influence of adsorbates and absorbates on surface segregation in the Pd−Pt system. LEIS measurements of polycrystalline $Pd_{20}Pt_{80}$ and $Pd_{80}Pt_{20}$ alloys have been carried out to determine the surface composition after heating in UHV, hydrogen (500 mbar), and oxygen (500 mbar).

3.1. Heating of the Pd−Pt Alloys in UHV. The atomic Pd surface fraction x_{Pd}^{surf} has been determined by LEIS as a function of the sample temperature in UHV (up to about 800 °C, which is the limit of the oven) for both the $Pd_{20}Pt_{80}$ and $Pd_{80}Pt_{20}$ alloys (see Figure 2). The samples were sputter cleaned at room temperature prior to each heat treatment and LEIS analysis. The atomic Pd surface fraction x_{Pd}^{surf} is measured while keeping the sample at the heating temperature for about 30 min. The Pd surface concentration increases with increasing temperature until at about 700 °C the Pd concentration does not change much and eventually slightly decreases. Such measurements of a sputter-cleaned alloy were repeated several times, and every time the same temperature dependence of x_{Pd}^{surf} was found. XPS measurements were performed after heating to 800 °C in UHV and contaminants were not detected.

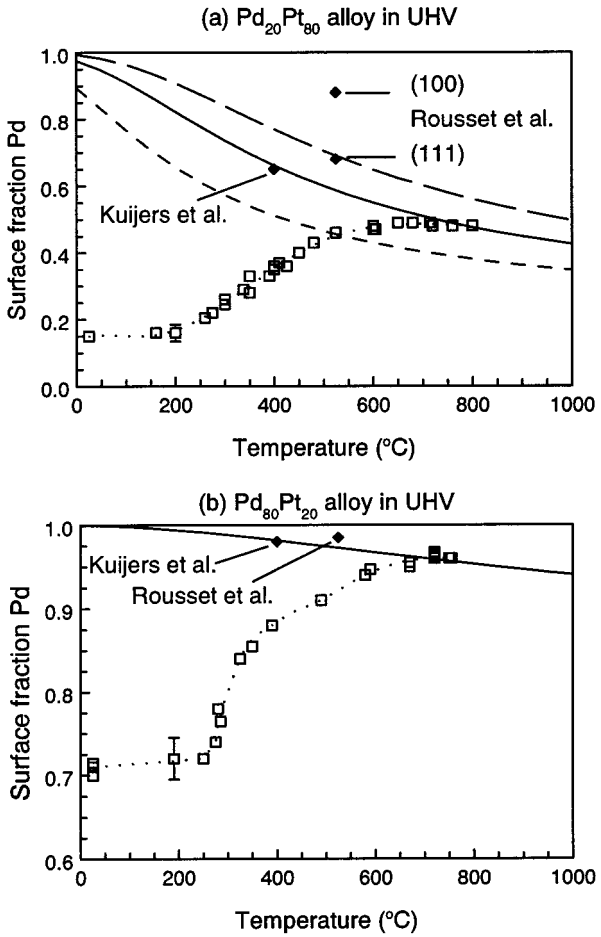

Figure 2. Atomic Pd surface fraction as a function of temperature of (a) the $Pd_{20}Pt_{80}$ alloy and (b) the $Pd_{80}Pt_{20}$ alloy heated in ultrahigh vacuum (UHV) for 30 min (measurements shown by the open squares; the dotted curve is to guide the eye and will be used in subsequent figures for comparison). The measured surface compositions are compared with the thermodynamic equilibrium composition based on eq 1 and the equilibrium compositions reported in the literature by Kuijers et al.[81] and Rousset et al.[82] The influence of the heat of segregation Q_{seg} on the equilibrium composition is illustrated in (a), where the long dashed curve corresponds to a Q_{seg} of 14.4 kJ/mol and the short dashed curve to 8 kJ/mol. Equilibrium is reached at about 700 °C, and the solid curve is the best fit for the equilibrium composition as a function of temperature, corresponding to a Q_{seg} of 11.5 kJ/mol for (a) and 14.5 kJ/mol for (b).

After sputtering at room temperature, x_{Pd}^{surf} is found by LEIS to be 0.15 and 0.70 for the $Pd_{20}Pt_{80}$ and $Pd_{80}Pt_{20}$ alloys, respectively. The small Pd depletion at the surface is due to preferential sputtering of Pd. The sputter yield (Y_i), i.e., the amount of atoms removed per impinging ion, is larger for Pd than for Pt. Using $Y_{Pd} = 2$ and $Y_{Pt} = 1.4$ for 3 keV Ne^+,[76] x_{Pd}^{surf} is expected to be 0.15 and 0.74 at the sputter equilibrium for the $Pd_{20}Pt_{80}$ and $Pd_{80}Pt_{20}$ alloys, respectively. This is in good agreement with the experimental values and explains the small Pd surface depletion after sputtering at room temperature. Our measured compositions are also in good agreement with previous work by Du Plessis et al. on the surface composition after sputtering with 1 keV Ar^+ ions.[75]

Heating of the Pd−Pt alloys results in Pd surface segregation (see Figure 2). The atomic Pd surface fraction x_{Pd}^{surf} increases with increasing temperature until thermodynamic equilibrium is reached. The surface composition at thermodynamic equilibrium can be described by the Langmuir−McLean expression:

$$\frac{x_{Pd}^{surf}}{x_{Pt}^{surf}} = \frac{x_{Pd}^{bulk}}{x_{Pt}^{bulk}} \exp\left(\frac{Q_{seg}}{RT}\right) \quad (1)$$

where Q_{seg} is the heat of segregation, which is the driving force for the surface segregation process. Here Q_{seg} is the energy it takes to exchange Pd surface atoms for Pt bulk atoms. It includes the change in surface free energy (γ_i), the heat of mixing (ΔH_{mix}), and the change in lattice strain energy:[5]

$$Q_{seg} = (\gamma_{Pt} - \gamma_{Pd})a + Q_{seg}^{mixing} + Q_{seg}^{strain} \quad (2)$$

where a is the molar surface area. For metals, γ can be approximated by using the heat of sublimation.[77,78] Since Pd and Pt have the same lattice structure (fcc) and almost the same lattice parameter (3.890 Å for Pd and 3.924 Å for Pt[79]), the lattice strain effect (Q_{seg}^{strain}) has been neglected for the Pd−Pt system. In the ideal solution model for surface segregation, Q_{seg}^{mixing} is also neglected. Since the surface free energy of Pd is smaller than that of Pt ($\gamma_{Pd} = 1.98$ J/m^2 and $\gamma_{Pt} = 2.43$ J/m^2 at 425 °C[80,81]), the ideal solution model indicates a Pd surface segregation in the Pd−Pt system as observed in our experiments. In the regular solution model, i.e., a pairwise bound model of the solid in combination with a broken bond model of the surface,[12] Q_{seg}^{mixing} is a function of the regular solution parameter Ω, which is equal to $\Delta H_{mix}/(x_{Pd}^{bulk} x_{Pt}^{bulk})$. Since the heat of mixing in the Pd−Pt system is slightly exothermic,[79] the regular solution model indicates a Pd surface segregation that is less pronounced than predicted by the ideal solution model.

To determine Q_{seg} experimentally, we assume that thermodynamic equilibrium is reached at 700−800 °C, because in this temperature range the Pd surface concentration does not increase anymore with increasing temperature and eventually slightly decreases. Since Pd segregates to the surface of the Pd−Pt system, i.e., $Q_{seg} > 0$, the equilibrium x_{Pd}^{surf} will decrease with increasing temperature according to eq 1. For Ni−Au and Ni−Pd alloys, having similar melting points, it was also found that thermodynamic equilibrium was reached at 700 °C.[18,20] Equation 1 was used to plot x_{Pd}^{surf} as a function of temperature for several values of Q_{seg} (see curves for the $Pd_{20}Pt_{80}$ alloy in Figure 2a). The value for Q_{seg} that results in the best fit of the data in the range 700−800 °C was chosen to describe the surface composition at thermodynamic equilibrium as a function of temperature. Using this procedure, we found that the heat of segregation $Q_{seg} = 11.5 \pm 0.5$ kJ/mol for the $Pd_{20}Pt_{80}$ alloy and $Q_{seg} = 14.5 \pm 0.5$ kJ/mol for the $Pd_{80}Pt_{20}$ alloy. The solid curves in Figure 2 show the estimated equilibrium surface composition as a function of temperature, assuming that Q_{seg} is independent of the sample temperature.

Estimates for Q_{seg} in the Pd−Pt system have been made by Chelikowsky[8] and by Tománek et al.,[17] using eq 2 with Q_{seg}^{mixing} equal to $^1/_3 f \cdot \Delta H_{mix}$ ($^1/_3$ represents the fraction of bonds that are broken at the surface, the factor f takes into account the deviation from the average crystal plane due to atomic relaxation and is equal to 0.71), as proposed by Miedema for dilute alloys.[13] A value of 27.5 ± 0.5 kJ/mol has been calculated, which would imply a much stronger Pd surface segregation than we found experimentally. Their approach to determine Q_{seg} is useful to make a qualitative prediction but most probably too simple to make a good quantitative prediction of surface segregation.

Kuijers et al.[81] have done AES measurements and used several segregation models to obtain the surface composition of Pd−Pt samples (powders and evaporated films) with different bulk compositions after equilibration at 400 °C for 16 h. Since AES measurements do not give direct information about the

first layer composition, they evaluated the AES data by Gallon's model.[81] They found a good agreement between theory and experiment, using a regular solution model with a variable parameter Ω to introduce the "nonregular behavior" of ΔH_{mix},[79] i.e., that the heat of mixing in the Pd−Pt system is dependent on the bulk composition. If we plot the equilibrium surface composition at 400 °C as predicted by Kuijers et al.[81] in Figure 2 for a $Pd_{20}Pt_{80}$ and $Pd_{80}Pt_{20}$ alloy, an excellent agreement with our equilibrium curve (solid curve) is found.

In recent work of Rousset et al.,[82] the first-layer compositions of (111) and (100) planes of Pd alloys at 525 °C have been calculated using an "advanced" broken-bond model, using the equivalent-medium approximation and bond-strength modifications at surfaces. The results for Pd−Pt alloys are shown in Figure 2. The calculated surface composition of the (111) plane is in reasonable agreement with our equilibrium curve (solid curve). The close-packed (111) plane is assumed to be dominant at the polycrystalline surface of our Pd−Pt alloys.

The difference between the measured surface composition and the equilibrium composition below 700 °C can be attributed to a slow metal atom diffusion and/or a depletion of Pd atoms in the subsurface region induced by sputter cleaning. The influence of both mechanisms on the segregation process will be discussed below. The formation of an ordered phase at the surface, which can be responsible for a deviation from the equilibrium composition (see, e.g., ref 21) for the Pd−Fe system), is excluded for the Pd−Pt system, since it forms a solid solution over the complete composition range.[79,83,84]

A low mobility of metal atoms in the Pd−Pt system may result in a slow Pd surface segregation. The mobility of surface atoms is generally larger than that of bulk atoms. Therefore, surface segregation is expected to be initiated by exchange between first- and second-layer atoms. At elevated temperatures also metal atom diffusion from bulk to surface layers will occur. In this case, our interpretation of the segregational behavior of the Pd−Pt system as shown in Figure 2 (dotted curve) is that exchange between first- and second-layer atoms may start to occur at about 250 °C and the kinetics of segregation determines the surface composition at elevated temperatures until equilibrium is reached at about 700 °C. Several models have been proposed to describe the kinetics of surface segregation.[10,85−88] We have used a model of Kristyan and Giber[89] to make a rough estimate of the diffusion coefficient of Pd in the $Pd_{20}Pt_{80}$ alloy. Using the measured x_{Pd}^{surf}, the equilibrium x_{Pd}^{surf}, and heating time (30 min), we found values for the diffusion coefficient in the order of $10^{-21}-10^{-22}$ m^2/s at 400−600 °C, comparable with values of $10^{-20}-10^{-24}$ m^2/s for bulk self-diffusion of Pd in a $Pd_{20}Pt_{80}$ alloy in this temperature range.[90]

Another explanation for the segregational behavior at $T <$ 700 °C could be that the surface composition is determined by the equilibration of a sputter-induced altered layer (see, e.g., refs 42 and 91). Due to extensive sputtering in order to clean the surface of the alloys, surface and near-surface layers can be altered significantly (several monolayers deep). A combination of preferential sputtering and radiation enhanced segregation[44] may result in a large Pd depletion in the altered layer of a sputter cleaned Pd−Pt alloy, as has been observed by Du Plessis et al.[75] Therefore, our interpretation of the segregational behavior of the Pd−Pt system as shown in Figure 2 (dotted curve) is that x_{Pd}^{surf} reflects the equilibrium between the first and second layer. The atomic Pd surface fraction x_{Pd}^{surf} is low due to the Pd depletion in the second layer and increases with temperature due to the increase of the Pd concentration in the second and deeper layers of the altered layer until equilibrium between first layer and bulk is reached at about 700 °C.

Most probably a combination of both mechanisms is responsible for the segregational behavior at $T <$ 700 °C, as indicated by the following experiments. The $Pd_{20}Pt_{80}$ alloy was heated at 400 °C in UHV for 24 h instead of 30 min. On the basis of the diffusion coefficient as discussed above, we expected to find a surface composition that is close to the equilibrium x_{Pd}^{surf} (about 0.66 at 400 °C); especially since Kuijers et al. reached thermodynamic equilibrium at 400 °C after a heat treatment of 16 h.[81] While x_{Pd}^{surf} was 0.36 after 30 min of heating in UHV, it increased to 0.44 after 24 h of heating in UHV, which is still not close to the equilibrium surface composition. This demonstrates that slow metal atom diffusion can only be partly the reason for the segregational behavior at $T <$ 700 °C. Kuijers et al. reached equilibrium at 400 °C probably due to a large concentration of defects in their Pd−Pt samples as obtained by their preparation procedure of the samples.[81]

In another experiment, the $Pd_{20}Pt_{80}$ alloy was heated to 800 °C to remove a possible altered layer and x_{Pd}^{surf} was measured during cooling to room temperature. During cooling, the atomic Pd surface fraction follows the equilibrium curve in the range 700−800 °C, but deviates from the equilibrium curve below 700 °C staying almost constant till room temperature. This provides evidence that the altered layer effect can only be partly the reason for the segregational behavior at $T <$ 700 °C. This experiment also clearly shows the influence of the treatment "history" on the alloy surface composition below the temperature where equilibrium is reached, as was e.g. nicely illustrated for Au−Ni alloys by Burton et al.[18,92]

Most of the surface science studies concerning surface segregation of bimetallic systems consider only treatments in UHV as shown above for the Pd−Pt system. However, the knowledge obtained from UHV studies cannot be used directly to predict surface segregation in supported bimetallic nanoclusters under reaction conditions. In addition, we have to know the influence of gas adsorption and absorption on surface segregation. In the next paragraphs we will discuss the influence of oxygen and hydrogen on surface segregation in Pd−Pt bulk alloys.

3.2. Heating of the Pd−Pt Alloys in Oxygen. The atomic Pd surface fractions x_{Pd}^{surf} have been determined by LEIS in the UHV main chamber after treatments of the $Pd_{20}Pt_{80}$ and $Pd_{80}Pt_{20}$ alloys at various temperatures in 500 mbar oxygen for 30 min in the prechamber of the ERISS setup. The results are shown in Figure 3 and compared with the equilibrium surface composition (solid curve) and the measured surface composition in UHV (dotted curve) as a function of temperature. The atomic Pd surface fraction is slightly higher after heating in oxygen than after heating in UHV, and it approaches the thermodynamic equilibrium composition already at about 400−500 °C. XPS measurements after the treatments in oxygen showed in some cases a small amount of carbon contamination. More contamination was found after treatments at temperatures of 600 °C or higher, deposited on the sample during and/or after treatment in the prechamber or segregated from the bulk to the surface of the alloy. Therefore, data obtained after treatments in the prechamber at temperatures above 550 °C were not included in this study. The presence of contaminants may influence surface segregation.[18−20] If the contaminants have a different interaction with Pd and Pt, enhanced segregation of the constituent with the highest affinity for the contaminant may occur. The small carbon contamination (detected by XPS) after oxygen treatments

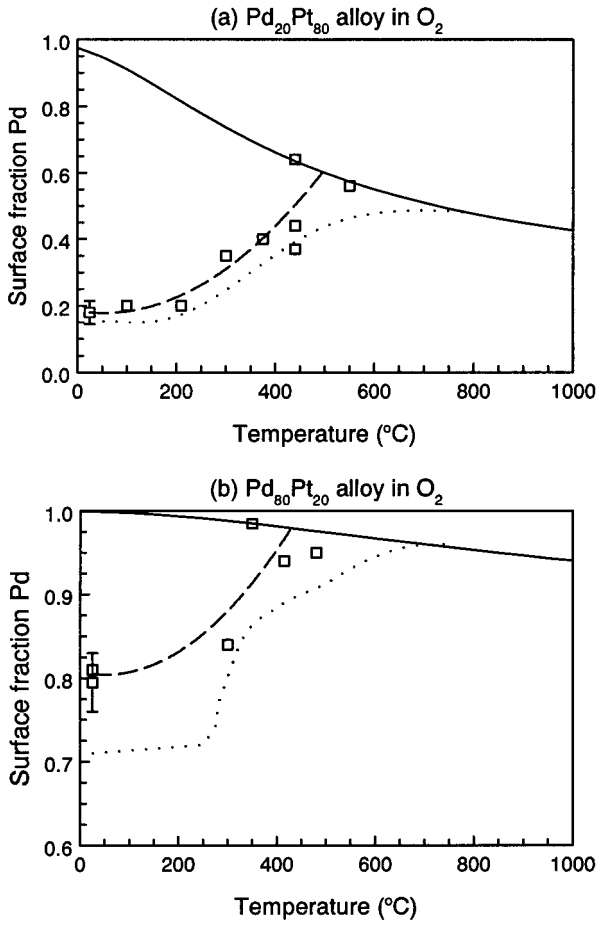

Figure 3. Atomic Pd surface fraction (measurements shown by squares on dashed curve) as a function of temperature for (a) the $Pd_{20}Pt_{80}$ alloy and (b) the $Pd_{80}Pt_{20}$ alloy heated in 500 mbar of oxygen for 30 min. The measured surface compositions are compared with the thermodynamic equilibrium composition (solid curves) and the measured surface composition after heating in UHV (dotted curves). The dashed curves are to guide the eye along the data points.

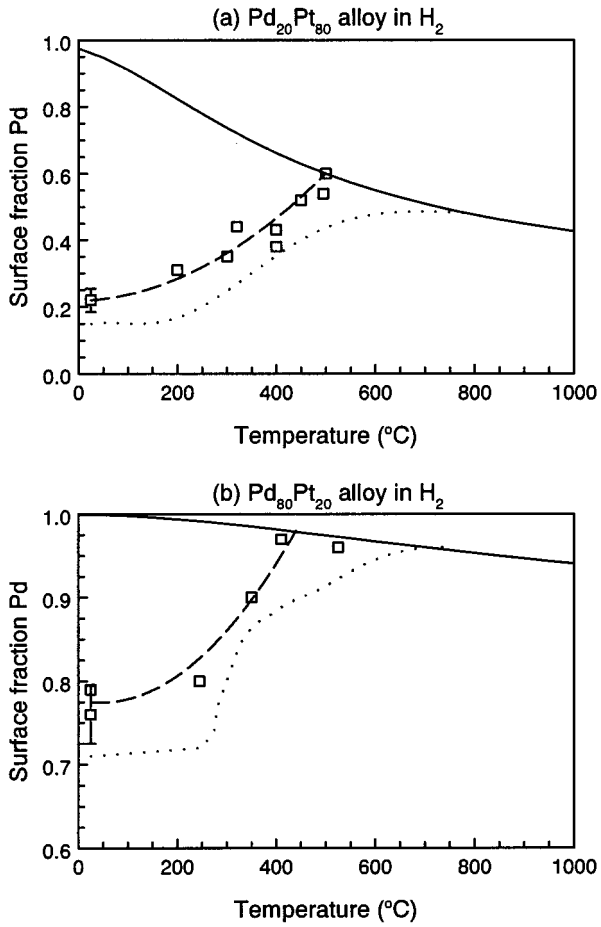

Figure 4. Atomic Pd surface fraction (squares on dashed curve) as a function of temperature of (a) the $Pd_{20}Pt_{80}$ alloy and (b) the $Pd_{80}Pt_{20}$ alloy heated in 500 mbar of hydrogen for 30 min. The measured surface compositions are compared with the thermodynamic equilibrium composition (solid curves) and the measured surface composition after heating in UHV (dotted curves). The dashed curves are to guide the eye along the data points.

of the alloys is not supposed to have a large influence on the surface composition of the Pd−Pt alloys.

Oxygen and other gases can influence the surface composition by chemisorption-induced surface segregation.[12,17,19] The difference in the chemisorption energy of an adsorbate on Pd and Pt has influence on the heat of segregation:

$$Q_{seg}^{chem} = Q_{seg} + \Delta H_{Pt}^{chem}\theta_{Pt} - \Delta H_{Pd}^{chem}\theta_{Pd} \qquad (3)$$

where θ_i is the adsorbate coverage on element *i*. The chemisorption energy of adsorbates on transition metals correlates linearly with the oxide formation energy.[93,94] Combining eqs 3 and 1, chemisorption-induced surface segregation will result in a new equilibrium curve with respect to surface segregation in UHV. In our case, the heat of adsorption of oxygen on Pd and Pt are the same, approximately 250 kJ/mol,[94,95] so we do not expect chemisorption-induced surface segregation in the Pd−Pt system by adsorption of oxygen.

Exposure to oxygen can also influence surface segregation in alloys when the constituents have different oxide-forming properties. For example, it was suggested for a Au−Ni alloy that not oxygen chemisorption but Ni oxide formation is the driving force for Ni surface segregation.[18,19] In the Pd−Pt system, it is expected that Pd oxidizes more readily than Pt.[96−98] So we suggest that Pd segregation may be enhanced by exposure to oxygen because of a lower activation energy for Pd−O bond formation in comparison to Pt−O bond formation, but the equilibrium composition is not changed by the presence of oxygen due to the similar Pd−O and Pt−O bond strengths.

3.3. Heating of the Pd−Pt Alloys in Hydrogen. The $Pd_{20}Pt_{80}$ and $Pd_{80}Pt_{20}$ alloys have also been exposed to 500 mbar of hydrogen for 30 min at various temperatures and the atomic Pd surface fractions x_{Pd}^{surf} have been determined by LEIS after these treatments. The results are shown in Figure 4 and compared with the equilibrium surface composition (solid curve) and the measured surface composition in UHV (dotted curve) as a function of temperature. The atomic Pd surface fraction is slightly higher after heating in hydrogen than after heating in UHV and it becomes equal to the thermodynamic equilibrium composition at about 400−500 °C, as was also found after treatments in oxygen (see section 3.2).

Carbon and sulfur contaminations have been detected by XPS after the hydrogen treatments. Most probably, the appearance of sulfur is due to hydrogen-enhanced segregation of sulfur as a bulk impurity to the surface of the alloys. As reported in the literature,[19] heating of metals such as Pd, Pt, Cu, and Mo in a hydrogen atmosphere gave rise to sulfur surface segregation probably due to the strong H−S bond, while heating without hydrogen did not result in the same sulfur segregation. A different interaction of sulfur with Pd and Pt is expected,[46,63,64,99] so we cannot exclude a possible role of the sulfur contamination in surface segregation in the Pd−Pt system. However, since

the amount of sulfur at the surface is estimated to be ≤0.1 ML, we believe that sulfur does not play a dominant role in the surface segregation process here. A combination of ion bombardment and hydrogen-enhanced surface segregation of bulk impurities may be a useful method to clean alloys.

We will now focus on the interaction of hydrogen with metals. Hydrogen chemisorbs dissociatively on transition metals. It can also be absorbed into subsurface positions, and it can diffuse deep into the bulk, where it is located on interstitial sites (α-hydride) and even can expand the metal lattice (β-hydride).[100−102] The high solubility of hydrogen in Pd is well-known, Pd hydride formation does occur and the amount of α-hydride and β-hydride depends on the temperature and hydrogen pressure.[100] Pt absorbs hydrogen but does not form a bulk metal hydride. Subsurface hydrogen states have been reported for Pt.[103−105] For alloys, hydrogen absorption depends on the composition, and it is different from the pure metals.[106] In Pd−Pt alloys, hydrogen absorption is reduced with increasing Pt content and β-hydride formation is completely surpressed for $x_{Pt}^{bulk} \geq 0.1-0.2$.[107,108]

Most probably, Pd surface segregation in the Pd−Pt alloys is enhanced by hydrogen absorption (see Figure 4). We believe that hydrogen adsorption will not result in chemisorption-induced surface segregation, because the heat of adsorption of hydrogen on Pd and Pt is the same, approximately 90 kJ/mol.[94,95] Tománek et al.[17] also suggested that hydrogen chemisorbed on the surface of an alloy does not induce much surface segregation, while hydrogen absorbed in the bulk can change the surface composition significantly. They illustrated this in a theoretical study of surface segregation in a Pd−Zr alloy, using a regular solution model that was modified to describe hydrogen absorption-induced surface segregation. In this method, the regular solution model was modified by adjusting the bond energies for the presence of subsurface hydrogen in the top surface layers of the alloy. Szabo et al.[109] used such a model, taking the top five surface layers into account, to estimate the influence of hydrogen absorption on the surface composition of Pd−Pt alloys (for $x_{Pd}^{bulk} = 0.15$ and 0.30). They predicted an increase in Pd surface segregation. Since they calculated for the topmost surface layer already a Pd surface fraction of 1 (at 525 °C) without the presence of hydrogen, in contrast to our results as presented in section 3.1, an increase of the Pd concentration in the second layer due to hydrogen absorption was proposed. This effect was more pronounced for the alloy with the higher Pd content due to the larger solubility of hydrogen. We note that this approach of hydrogen absorption-induced surface segregation also results in an equilibrium composition that is different from equilibrium in UHV. Our experiments do not indicate that this is the case.

Another mechanism of hydrogen absorption-enhanced segregation in Pd−Pt alloys may be responsible for the enhanced Pd surface segregation. In metallurgical studies of Flanagan and co-workers,[110−112] a so-called hydrogen-induced lattice migration (HILM) was proposed and observed to occur after exposure of Pd alloys to high hydrogen pressures and moderate temperatures. They found that a $Pd_{90}Pt_{10}$ alloy separates partially into Pd-rich and Pt-rich regions after exposure to 5.5 MPa hydrogen at 175 °C for several days. The authors suggested that absorbed hydrogen catalyzes metal atom diffusion here. The enhanced diffusion of metal atoms may be caused by a copious hydrogen absorption-induced vacancy formation, as was shown and discussed for Ni−Pd alloys.[113,114] Since we use a much lower hydrogen pressure in our experiments, it is not expected for our samples that a HILM mechanism will result in phase separation as described above but may result in enhanced Pd surface segregation to the same equilibrium composition as obtained by heating in UHV by a faster metal atom diffusion in the (sub)surface layers, enhanced by absorbed hydrogen.

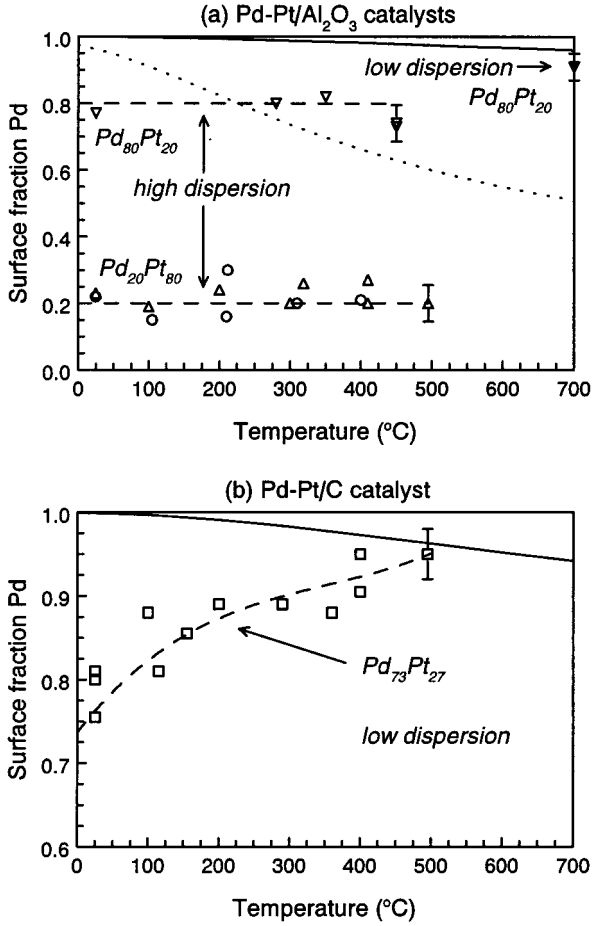

Figure 5. Atomic Pd surface fraction as a function of temperature of (a) the alumina-supported Pd−Pt catalysts with a high (*D* close to 1) and low metal dispersion (0.8) and (b) the carbon-supported Pd−Pt catalysts with a metal dispersion of 0.3. The spheres in (a) show the measured surface compositions of the $Pd_{20}Pt_{80}/Al_2O_3$ catalyst after treatment in 500 mbar oxygen for 30 min. The other markers (triangles in (a), squares in (b)) indicate the surface composition after treatments of the catalysts in 500 mbar of hydrogen for 30 min. The solid curves show the equilibrium surface composition as a function of temperature as calculated with $Q_{seg} = 14.5$ kJ/mol and a bulk Pd fraction of 0.8 in (a) and 0.73 in (b). The dotted curve in (a) represents the calculated equilibrium surface composition for $Q_{seg} = 11.5$ kJ/mol and a bulk Pd fraction of 0.2. The dashed curves are to guide the eye along the data points.

4. Results and Discussion of Surface Segregation in Pd−Pt Nanoclusters

4.1. Metal Surface Composition of Pd−Pt Catalysts. The atomic Pd surface fractions of supported Pd−Pt nanoclusters have been determined with LEIS, using about 2×10^{13} Ne^+ ions/cm^2 per measurement, after treatments in hydrogen and oxygen (500 mbar) at various temperatures. We note that the LEIS measurements provide the surface composition of the supported Pd−Pt clusters on the outside of the catalysts sample. Clusters in pores are not probed by LEIS. We assume that the measured surface composition represents the (average) surface composition of all clusters in the catalyst. The results are shown in Figure 5, including the equilibrium surface composition as

calculated for bulk alloys (solid curves). The Pd-rich catalysts were treated only in hydrogen, since phase separation of Pd-rich bimetallic clusters into PdO clusters and Pt-rich clusters may occur by treatment in oxygen at $T \geq 300$ °C.[97]

The results of the alumina supported catalysts are shown in Figure 5a. The surface compositions of the highly dispersed Pd−Pt/Al_2O_3 catalysts (with a metal dispersion close to 1) are equal within experimental error to the bulk compositions. The absence of surface segregation was also mentioned in the literature for highly dispersed silica supported Pd−Pt catalysts, indicated by results of kinetic studies[55] and by infrared spectroscopy.[115] This is completely different from the segregational behavior in the Pd−Pt alloys, where the surface composition clearly deviates from the bulk composition due to Pd surface segregation (see Figures 3 and 4). In contrast to these results for highly dispersed catalysts, Pd surface segregation was observed in LEIS measurements of the $Pd_{80}Pt_{20}/Al_2O_3$ catalyst with a lower metal dispersion of about 0.8, which shows the importance of the cluster size in the surface segregation process. This catalyst with a total metal loading of 3.3 wt % was treated in hydrogen at 700 °C (at the SRTCA) in order to obtain the lower metal dispersion. The catalyst was transferred through air to the LEIS setup and measured without performing any pretreatment and also measured after a hydrogen treatment at 400 °C. In both cases, a clear Pd surface segregation was found resulting in a surface composition ($x_{Pd}^{surf} = 0.91$) that approaches thermodynamic equilibrium (see Figure 5a).

Figure 5b shows the surface compositions of the $Pd_{73}Pt_{27}$/C catalyst after treatments in hydrogen. This catalyst has a metal dispersion of about 0.3. A clear Pd surface enrichment was found for the carbon-supported catalyst after treatment in hydrogen, which increases with increasing temperature. Atomic Pd surface fractions of 0.9−0.95 were measured after hydrogen treatments at 400−500 °C, which are close to the thermodynamic equilibrium surface fraction of 0.97 and 0.96 at 400 and 500 °C, respectively, as calculated with eq 1 using $Q_{seg} = 14.5$ kJ/mol. The measured atomic Pd fraction is constant within experimental error upon increasing the ion dose up to approximately 2×10^{14} Ne^+ ions/cm^2, but the Pd fraction decreases if the ion dose becomes higher. When sputtering the hydrogen-treated $Pd_{73}Pt_{27}$/C catalyst with an ion dose of about 10^{16} Ne^+/cm^2 or more, an atomic Pd fraction of 0.73 was always found by LEIS, which equals the atomic Pd bulk fraction. There are at least three processes that determine together the surface composition after prolonged exposure of the catalysts to the ion beam: (1) preferential sputtering, which leads to a slightly lower Pd surface concentration as observed on bulk alloys; (2) destruction of the clusters by the ion beam, which results in a redistribution of the clusters over the support and should yield a surface composition equal to the bulk composition; (3) the exposure of clusters that were not previously visible to the ion beam, which again contribute a Pd-enriched surface. Apparently, prolonged sputtering results here in the average atomic Pd fraction being exposed to the ion beam, but it is not possible to extract from the measurements the importance of each of the above-mentioned processes to the final surface composition. Once more, we would like to emphasize that all measurements on the supported clusters directly after the pretreatment are performed at such a low ion dose that these processes do not have a significant influence on the surface composition analysis (see section 2.2).

The surface composition of the supported Pd−Pt nanoclusters is influenced by several parameters. In the next paragraphs, we will discuss the influence of hydrogen and oxygen, cluster size, and metal−support interaction on surface segregation in Pd−Pt nanoclusters in general in order to find out which parameter(s) give rise to the difference in segregation here between alloys and some of the measured catalysts.

4.2. Effect of Adsorbates/Absorbates on Surface Segregation in Pd−Pt Nanoclusters. As was shown for the alloys in sections 3.2 and 3.3, oxygen and hydrogen can have a significant influence on surface segregation in the Pd−Pt system. Chemisorption-induced surface segregation by oxygen and hydrogen is excluded for the Pd−Pt system, since the heats of adsorption of oxygen and hydrogen on Pd and Pt are (almost) the same for both metals. However, other processes in which oxygen or hydrogen are involved can affect surface segregation and may be different for alloys and supported nanoclusters, as will be discussed in this section.

The oxide-forming properties of the constituents are different for Pd and Pt which can result in enhanced Pd surface segregation in Pd−Pt alloys. In the case of small supported bimetallic particles, the difference in oxide formation of the constituents can eventually result in phase separation.[116] Chen and Schmidt[97] studied Pd−Pt particles of about 5−10 nm evaporated on a flat SiO_2 model support using scanning transmission electron microscopy. They showed that phase separation of the Pd−Pt particles into PdO particles and Pt-rich particles occurs after heating in air for 1 h at $T \geq 300$ °C for particles with compositions of $x_{Pd} \geq 0.6$ and at $T \geq 600$ °C for particles with a composition of $x_{Pd} = 0.2$. All measurements previously reported for the Pt-rich catalyst were obtained below the phase separation temperature, and we did not study Pd-rich catalysts treated in oxygen. Therefore, we do not expect that phase separation occurs in our experiments. In one case we also studied a $Pd_{80}Pt_{20}/Al_2O_3$ catalyst that was calcined at 450 °C in air, while usually the calcination temperature is about 300−320 °C, and phase separation was clearly observed by electron microscopy. LEIS measurements also indicated a change in surface composition and/or structure: an atomic Pd surface fraction of 0.6−0.65 was found, lower than the atomic Pd bulk fraction.

Pd surface segregation in Pd−Pt alloys can be enhanced by hydrogen absorption. In the case of small supported bimetallic particles, the hydrogen solubility may be considerably different from that in bulk alloys. It has been found for Pd catalysts that the solubility of hydrogen in Pd particles decreases with increasing dispersion.[117−120] Although a lower hydrogen solubility in the nanoclusters may result in less Pd surface segregation, this will not give rise to a complete suppression of Pd surface segregation in Pd−Pt nanoclusters, since heat treatments without hydrogen (in UHV) still result in a considerable Pd surface segregation in the Pd−Pt alloys (see Figure 2).

Since hydrogen and oxygen treatments do not result in surface segregation in the supported catalysts with very small Pd−Pt clusters but do give rise to surface segregation in the catalysts with larger Pd−Pt clusters to approximately the same extent as in the bulk alloys, we believe that with respect to the alloys the effect of hydrogen and oxygen on surface segregation in Pd−Pt nanoclusters is not large.

4.3. Effect of Cluster Size on Surface Segregation in Pd−Pt Nanoclusters. In contrast to the bulk alloys, small metal clusters contain a limited amount of metal atoms and the surface atoms of nanoclusters will be less coordinated than surface atoms of bulk alloys. Both differences between alloys and nanoclusters can have a significant effect on the surface segregation process.

As indicated by the larger atomic Pd surface fraction of the more open (100) plane in comparison to that of the close packed

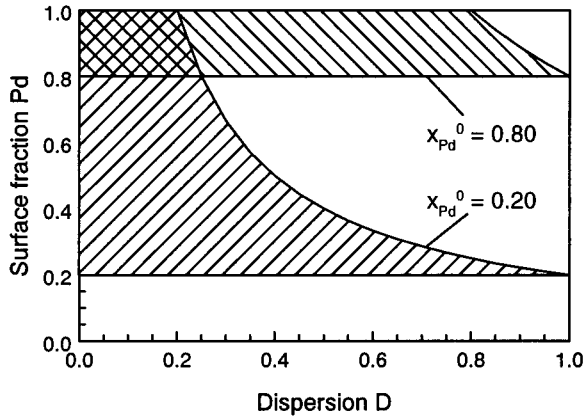

Figure 6. Illustration of the cluster size effect (limited supply of atoms) on surface segregation. The dashed areas indicate the possible atomic Pd surface fractions in Pd−Pt nanoclusters with an overall bulk composition of $x_{Pd}^0 = 0.20$ and 0.80 as a function of the dispersion.

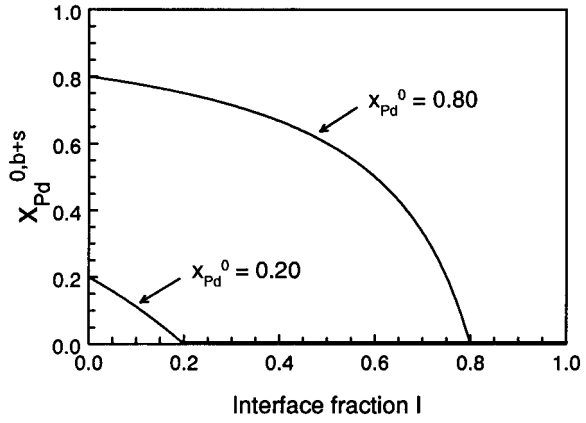

Figure 7. Illustration of the effect of preferential Pd adsorption at the metal−support interface ($x_{Pd}^{int} = 1$) on the average atomic Pd fraction in the rest of a supported Pd−Pt cluster ($x_{Pd}^{0,b+s}$) for $x_{Pd}^0 = 0.20$ and 0.80 as a function of the fraction of metal atoms in contact with the support (*I*).

(111) plane of the Pd−Pt alloys (as reported by Rousset et al.,[82] see Figure 2a), the reduced coordination of surface atoms of Pd−Pt nanoclusters may give rise to an enhanced Pd surface segregation that is most pronounced for the smallest clusters. However, we found the opposite result: Pd surface segregation is completely absent in the highly dispersed Pd−Pt clusters, while in the low-dispersed catalysts Pd surface segregation takes place to approximately the same extent as in the Pd−Pt alloy (see Figure 4b). Therefore, we conclude that the reduced coordination of the surface atoms of the Pd−Pt clusters is not an important parameter for surface segregation here.

Enhanced Pd segregation to sites on the cluster with a reduced coordination (e.g., corner sites) may still occur, as was calculated for Pd−Pt clusters by Rousset et al.[121,122] This site segregation may be of great importance for the catalytic performance if these low-coordinated sites are the active sites of the catalyst. If the fraction of low coordination sites is small, site segregation in supported clusters cannot be detected by LEIS because it gives only the average surface composition of the clusters.

Surface segregation can be strongly surpressed by a limited supply of atoms to the surface in systems with a relative large number of surface atoms, such as nanoclusters[12,22,23,25] and thin films.[123,124] This effect may have a significant influence on the surface composition of the Pd−Pt catalysts. The metal dispersion of the catalysts (*D*), i.e., the number of metal surface atoms divided by the total number of metal atoms, determines whether such a cluster size effect is important for the surface segregation process. This can be illustrated by the Pd mass balance for a Pd−Pt cluster with dispersion *D*:[12]

$$x_{Pd}^0 = x_{Pd}^{surf} D + x_{Pd}^{bulk}(1 - D) \qquad (4)$$

where x_{Pd}^0 is the overall atomic Pd bulk fraction of a cluster, x_{Pd}^{bulk} is the atomic Pd fraction of the inner (bulk) atoms of the cluster, and x_{Pd}^{surf} is the atomic Pd fraction of the cluster surface. Assuming Pd surface segregation, the boundary conditions are $x_{Pd}^0 \le x_{Pd}^{surf} \le 1$ and $0 \le x_{Pd}^{bulk} \le x_{Pd}^0$. The dashed areas in Figure 6 give all the possible values of x_{Pd}^{surf} as a function of the dispersion *D* that can be obtained by Pd surface segregation in nanoclusters (for $x_{Pd}^0 = 0.20$ and 0.80), as determined by eq 4 and the boundary conditions. Figure 6 will be used now to give an explanation for the surface segregational behavior in Pd−Pt nanoclusters.

The Pd−Pt nanoclusters that are highly dispersed over the γ-alumina support have a metal dispersion that is close to 1. As indicated by Figure 6, the maximum equilibrium composition that can be reached is close to the bulk composition due to the limited supply of Pd atoms from the bulk to the cluster surface. For the lower dispersed catalysts, a $Pd_{80}Pt_{20}/Al_2O_3$ and $Pd_{73}Pt_{27}/C$ catalyst with a metal dispersion of about 0.8 and 0.3, respectively, we do not expect a cluster size effect on the surface composition on the basis of Figure 6. These predictions for surface segregation in high- and low-dispersed Pd−Pt catalysts are in good agreement with the experimental results (see Figure 5). So the cluster size effect as discussed above explains the surface segregational behavior in the Pd−Pt nanoclusters.

4.4. Effect of Metal−Support Interaction on Surface Segregation in Pd−Pt Nanoclusters. Surface segregation in supported bimetallic clusters can be altered by preferential adsorption of one of the constituents at the metal−support interface.[22] If, e.g., Pd segregates to the metal−support interface and preferentially binds to the support as was suggested for Pd−Pt/Al_2O_3 catalysts by Haro et al.,[125] Pd segregation to the surface of the clusters may be reduced. This can also be illustrated with a Pd mass balance, in a similar way as done in section 4.3 by eq 4. For a supported Pd−Pt cluster with a dispersion *D* and a fraction *I* of metal atoms in contact with the support, i.e., the number of metal atoms at the interface divided by the total number of metal atoms, the mass balance is

$$x_{Pd}^0 = x_{Pd}^{surf} D + x_{Pd}^{bulk}(1 - D - I) + x_{Pd}^{int} I \qquad (5)$$

where x_{Pd}^{int} is the atomic Pd fraction at the metal−support interface. The fraction *I* depends on the particle shape, e.g., supported hemispherical particles have a surface to interface area ratio of 2, so *I* is approximately $^1/_2 D$ for low dispersions. If no preferential metal adsorption at the metal−support interface occurs, x_{Pd}^{int} is equal to x_{Pd}^{bulk} and eq 5 becomes equal to eq 4. If Pd atoms tend to accumulate at the interface, the average atomic Pd fraction in the rest of the cluster (indicated by $x_{Pd}^{0,b+s}$) decreases with the consequence that Pd surface segregation will be reduced and $x_{Pd}^{0,b+s}$ can even become 0 if *I* is high enough. This is shown in Figure 7 for $x_{Pd}^0 = 0.20$ and 0.80 in the extreme case when all the metal atoms at the metal−support interface are Pd atoms ($x_{Pd}^{int} = 1$). Figure 7 also demonstrates that for the low-dispersed Pd-rich catalysts the effect of preferential Pd adsorption at the metal−support interface does not significantly influence Pd surface segregation because $x_{Pd}^{0,b+s}$ is only slightly reduced.

The influence of metal−support interactions (MSI) on the properties and performance of a catalyst has been the topic of

many studies; however, it is still not possible to predict the MSI strength accurately. Both Pd and Pt have a fairly strong interaction with an alumina support (see, e.g., refs 126−132). At temperatures above 500 °C under reducing conditions, even Pt−Al[133−135] and Pd−Al[136,137] alloy formation have been suggested. Venezia et al.[138,139] observed a shift of 0.5 eV to lower binding energies by XPS for the Pd 3d and Pt 4f peaks of pumice-supported Pd−Pt catalysts and attributed this to the presence of a metal−support interaction. For an α-alumina-supported Pd catalyst a large interaction between metal and support has been assumed to cause a binding energy shift of about 1 eV to higher binding energies.[140] We have performed XPS measurements at SRTCA, using an ESCALAB 220i-XL spectrometer, to look for similar effects in the highly dispersed alumina-supported catalysts. However, we did not observe any shift due to MSI. Pd and Pt are most probably bonded to the oxygen of the alumina support. As has been discussed in section 3.2, Pd has a higher affinity for oxygen than Pt, but we do not expect that the difference is so large that Pd preferentially adsorbs on the metal−support interface and prevents Pd surface segregation.

It is also believed that the interaction of Pd and Pt with the carbon support does not differ significantly to affect surface segregation. The interaction of transition metals to a carbon support is generally supposed to be weaker than the metal−alumina interaction.[141] This may give rise to sintering of the bimetallic clusters on the carbon support at elevated temperatures and an increase of the cluster size. The effect of the cluster size on surface segregation was discussed in section 4.3. We believe that the cluster size effect is the main reason for the differences in surface segregation in the Pd−Pt alloys and alumina- and carbon-supported catalysts. It is shown that the presence of hydrogen and oxygen and MSI plays only a marginal role in the surface segregation process in the supported nanoclusters discussed here.

5. Conclusions

Low-energy ion scattering (LEIS) is a suitable technique to determine the metal surface composition of supported bimetallic catalysts and alloys. The surface composition of these systems can be influenced by the temperature, the presence of hydrogen and oxygen, metal−support interactions, and the cluster size.

In Pd−Pt alloys, Pd surface segregation takes place and increases with increasing temperature. In ultrahigh vacuum, thermodynamic equilibrium is reached at about 700 °C. Treatments in hydrogen or oxygen result in an enhanced Pd surface segregation and thermodynamic equilibrium is reached at 400−500 °C. The surface composition of very small Pd−Pt nanoclusters in bimetallic catalysts is different from that of the Pd−Pt alloys with the same bulk composition, after exposure to hydrogen or oxygen at elevated temperatures (up to 400−500 °C). The Pd−Pt cluster size clearly influences surface segregation while the effect of hydrogen and oxygen and MSI on surface segregation in the supported Pd−Pt catalysts is not significant here. For highly dispersed Pd−Pt catalysts with a metal dispersion close to 1, surface segregation is completely surpressed due to a limited supply of Pd atoms from the bulk to the surface of the nanoclusters. For Pd−Pt catalysts with a low metal dispersion of about 0.3 and 0.8, Pd surface segregation does take place to approximately the same extent as in the Pd−Pt bulk alloys.

Acknowledgment. Ir. Noud van den Broek (Lab. for Inorganic Chemistry and Catalysis, Faculty of Chemical Engineering, Eindhoven University of Technology) is acknowledged for performing the hydrogen chemisorption measurements. The investigations described in this paper were supported by The Netherlands Technology Foundation (STW).

References and Notes

(1) Sinfelt, J. H. *Bimetallic catalysts: discoveries, concepts and applications*; Exxon Monograph; John Wiley & Sons: New York, 1983.
(2) Ponec, V.; Bond, G. C. *Catalysis by metals and alloys*; Studies in surface science and catalysis; Elsevier: Amsterdam, 1995; Vol. 95.
(3) Campbell, C. T. *Annu. Rev. Phys. Chem.* **1990**, *41*, 775.
(4) Rodriguez, J. A. *Surf. Sci. Rep.* **1996**, *24*, 223.
(5) Wynblatt, P.; Ku, R. C. *Surf. Sci.* **1977**, *65*, 511.
(6) Johnson, W. C., Blakely, J. M., Eds. *Interfacial segregation*; American Society for Metals: Metals Park, OH, 1979.
(7) Sachtler, W. M. H.; van Santen, R. A. *Appl. Surf. Sci.* **1979**, *3*, 121.
(8) Chelikowsky, J. R. *Predictions for surface segregation in 2.550 binary intermetallic alloys*; research report; Exxon Research and Engineering Co.: Linden, NJ.
(9) Ossi, P. M. *Surf. Sci.* **1988**, *201*, L519.
(10) du Plessis, J. *Surface segregation*; Solid State Phenomena; Sci-Tech Publications: Vaduz, Liechtenstein, 1990; Vol. 11.
(11) Somorjai, G. A. *Introduction to surface chemistry and catalysis*; John Wiley & Sons: New York, 1994; p 271.
(12) Williams, F. L.; Nason, D. *Surf. Sci.* **1974**, *45*, 377.
(13) Miedema, A. R. *Z. Metallk.* **1978**, *69*, 455.
(14) Hamilton, J. C. *Phys. Rev. Lett.* **1979**, *42*, 989.
(15) Abraham, F. F.; Brundle, C. R. *J. Vac. Sci. Technol.* **1981**, *18*, 506.
(16) Mukherjee, S.; Morán-López, J. L. *Surf. Sci.* **1987**, *189/190*, 1135.
(17) Tománek, D.; Mukherjee, S.; Kumar, V.; Bennemann, K. H. *Surf. Sci.* **1982**, *114*, 11.
(18) Burton, J. J.; Helms, C. R.; Polizzotti, R. S. *J. Chem. Phys.* **1976**, *65*, 1089.
(19) Latta, E. E.; Bonzel, H. P. In *Interfacial segregation*; Johnson, W. C., Blakely, J. M., Eds.; American Society for Metals: Metals Park, OH, 1979; p 381.
(20) Tang, S.; Lam, N. Q. *Surf. Sci.* **1989**, *223*, 179.
(21) Creemers, C. *Surf. Sci.* **1996**, *360*, 10.
(22) Gijzeman, O. L. J. *Appl. Surf. Sci.* **1993**, *64*, 9.
(23) Helms, C. R. In *Interfacial segregation*; Johnson, W. C., Blakely, J. M., Eds.; American Society for Metals: Metals Park, OH, 1979; p 175.
(24) Morán-López, J. L.; Falicov, L. M. *Surf. Sci.* **1979**, *79*, 109.
(25) Groomes, D. O.; Wynblatt, P. *Surf. Sci.* **1985**, *160*, 475.
(26) Kelley, M. J.; Dadyburjor, D. B. In *Catalyst deactivation*; Petersen, E. E., Bell, A. T., Eds.; Chemical Industries; Marcel Dekker: New York, 1987; Vol. 30, p 125.
(27) Katrib, A.; Petit, C.; Légaré, P.; Hilaire, L.; Maire, G. *Surf. Sci.* **1987**, *189/190*, 886.
(28) Juszczyk, W.; Karpiński, Z.; Łomot, D.; Pielaszek, J.; Sobczak, J. W. *J. Catal.* **1995**, *151*, 67.
(29) Zsoldos, Z.; Garin, F.; Hilaire, L.; Guczi, L. *J. Mol. Catal.* **1996**, *A 111*, 113.
(30) Gonzalez, R. D. *Appl. Surf. Sci.* **1984**, *19*, 181.
(31) Sinfelt, J. H. *Acc. Chem. Res.* **1987**, *20*, 134.
(32) Santra, A. K.; Subbanna, G. N.; Rao, C. N. R. *Surf. Sci.* **1994**, *317*, 259.
(33) Rades, T.; Pak, C.; Polisset-Thfoin, M.; Ryoo, R.; Fraissard, J. *Catal. Lett.* **1994**, *29*, 91.
(34) Sault, A. G. *Catal. Lett.* **1994**, *29*, 145.
(35) Niehus, H.; Heiland, W.; Taglauer, E. *Surf. Sci. Rep.* **1993**, *17*, 213.
(36) Brongersma, H. H.; Sparnaay, M. J.; Buck, T. M. *Surf. Sci.* **1978**, *71*, 657.
(37) Varga, P.; Hetzendorf, G. *Surf. Sci.* **1985**, *162*, 544.
(38) Hoflund, G. B.; Asbury, D. A.; Kirszensztejn, P.; Laitinen, H. A. *Surf. Sci.* **1985**, *161*, L583.
(39) Overbury, S. H.; van den Oetelaar, R. J. A.; Zehner, D. M. *Phys. Rev.* **1993**, *B48*, 1718.
(40) Bertolini, J. C.; Rousset, J. L.; Miegge, P.; Massardier, J.; Tard, B.; Samson, Y.; Khanra, B. C.; Creemers, C. *Surf. Sci.* **1993**, *281*, 102.
(41) den Otter, W. K.; Brongersma, H. H.; Feil, H. *Surf. Sci.* **1994**, *306*, 215.
(42) Lam, N. Q.; Wiedersich, H. *Nucl. Instrum. Methods* **1987**, *B18*, 471.
(43) Shimizu, R. *Nucl. Instrum. Methods* **1987**, *B18*, 486.
(44) Kelly, R. *Nucl. Instrum. Methods* **1989**, *B39*, 43.
(45) McKee, D. W.; Norton, F. J. *J. Catal.* **1964**, *3*, 252.
(46) Kovach, S. M.; Wilson, G. D. United States Patent 3,943,053, 1976.

(47) Ruiz-Vizcaya, M. E.; Novaro, O.; Ferreira, J. M.; Gómez, R. *J. Catal.* **1978**, *51*, 108.
(48) Grill, C. M.; Gonzalez, R. D. *J. Catal.* **1980**, *64*, 487.
(49) Miner, R. S.; Namba, S.; Turkevich, J. *Stud. Surf. Sci. Catal.* **1981**, *7*, 160.
(50) Toshima, N. *J. Macromol. Sci.−Chem.* **1990**, *A27*, 1225.
(51) Deng, Y.; An, L. *Appl. Catal.* **1994**, *A119*, 13.
(52) Deganello, G.; Duca, D.; Liotta, L. F.; Martorana, A.; Venezia, A. M.; Benedetti, A.; Fagherazzi, G. *J. Catal.* **1995**, *151*, 125.
(53) Skoglundh, M.; Löwendahl, L. O.; Ottersted, J.-E. *Appl. Catal.* **1991**, *77*, 9.
(54) Vigneron, S.; Deprelle, P.; Hermia, J. *Catal. Today* **1996**, *27*, 229.
(55) Karpiński, Z.; Kościelski, T. *J. Catal.* **1980**, *63*, 313.
(56) Koscielski, T.; Karpinski, Z.; Paál, Z. *J. Catal.* **1982**, *77*, 539.
(57) Margitfalvi, J.; Szabó, S.; Nagy, F.; Göbölös, S.; Hegedüs, M. In *Preparation of catalysts III*; Poncelet, G., Grange, P., Jacobs, P. A., Eds.; Elsevier: Amsterdam, 1983; p 473.
(58) van de Moesdijk, C. G. M. Ph.D. Thesis, Eindhoven University of Technology, The Netherlands, 1979.
(59) Gosser, L. W.; Schwartz, J.-A. T. U.S. Patent 4,832,938, 1989.
(60) Nagashima, H.; Ishiuchi, Y.; Hiramatsu, Y. U.S. Patent 5,236,692, 1993.
(61) Attard, G. A.; Price, R. *Surf. Sci.* **1995**, *335*, 63.
(62) Ramesh, K. V.; Sarode, P. R.; Vasudevan, S.; Shukla, A. K. *J. Electroanal. Chem.* **1987**, *223*, 91.
(63) Ghazi, M. *C. R. Acad. Sci. Paris* **1990**, t.310, Ser. II, 1415.
(64) Lin, T.-B.; Jan, C.-A.; Chang, J.-R. *Ind. Eng. Chem. Res.* **1995**, *34*, 4284.
(65) Darji, R.; Howie, A. EMAG '95, Institute of Physics conference series; IOP Publishing: Bristol, UK, 1995; Vol. 147, p 207.
(66) Kip, B. J.; Duivenvoorden, F. B. M.; Koningsberger, D. C.; Prins, R. *J. Catal.* **1987**, *105*, 26.
(67) Scholten, J. J. F.; Pijpers, A. P.; Hustings, A. M. L. *Catal. Rev.-Sci. Eng.* **1985**, *27*, 151.
(68) Hellings, G. J. A.; Ottevanger, H.; Boelens, S. W.; Knibbeler, C. L. C. M.; Brongersma, H. H. *Surf. Sci.* **1985**, *162*, 913.
(69) Ackermans, P. A. J.; van der Meulen, P. H. F. M.; Ottevanger, H.; van Straten, F. E.; Brongersma, H. H. *Nucl. Instrum. Methods* **1988**, *B 35*, 541.
(70) Bergmans, R. H. Ph.D. Thesis, Eindhoven University of Technology, The Netherlands, 1996; p 55.
(71) Nooij, O. W. Master Thesis, Eindhoven University of Technology, The Netherlands, 1995.
(72) Taglauer, E.; Heiland, W.; Beitat, U. *Surf. Sci.* **1979**, *89*, 710.
(73) Ackermans, P. A. J.; Krutzen, G. C. R.; Brongersma, H. H. *Nucl. Instrum. Methods* **1990**, *B45*, 384.
(74) van den Oetelaar, L. C. A.; van Benthem, H. E.; Helwegen, J. H. J. M.; Stapel, P. J. A.; Brongersma, H. H., submitted to *Surf. Interface Anal.*
(75) Du Plessis, J.; van Wyk, G. N.; Taglauer, E. *Surf. Sci.* **1989**, 220, 381.
(76) Matsunami, N.; Yamamura, Y.; Itikawa, Y.; Itoh, N.; Kazumata, Y.; Miyagawa, S.; Morita, K.; Shimizu, R.; Tawara, H. *At. Data Nucl. Data Tables* **1984**, *31*, 1.
(77) van Santen, R. A.; Sachtler, W. M. H. *J. Catal.* **1974**, *33*, 202.
(78) Overbury, S. H.; Bertrand, P. A.; Somorjai, G. A. *Chem. Rev.* **1975**, *75*, 547.
(79) Darby, J. B.; Myles, K. M. *Metall. Trans.* **1972**, *3*, 653.
(80) Tyson, W. R.; Miller, W. A. *Surf. Sci.* **1977**, *62*, 267.
(81) Kuijers, F. J.; Tieman, B. M.; Ponec, V. *Surf. Sci.* **1978**, *75*, 657.
(82) Rousset, J. L.; Bertolini, J. C.; Miegge, P. *Phys. Rev.* **1996**, *B53*, 4947.
(83) Massalski, T. W., Murray, J. L., Bennet, L. H., Baker, H., Eds.; *Binary alloy phase diagrams*; American Society for Metals: Metals Park, OH, 1986; p 1863.
(84) Lu, Z. W.; Klein, B. M. *J. Phase Equilibria* **1995**, *16*, 36.
(85) Lea, C.; Seah, M. P. *Philos. Mag.* **1977**, *35*, 213.
(86) Hofmann, S.; Erlewein, J. *Surf. Sci.* **1978**, *77*, 591.
(87) Mervyn, D. A.; Baird, R. J.; Wynblatt, P. *Surf. Sci.* **1979**, *82*, 79.
(88) Sparnaay, M. J.; Thomas, G. E. *Surf. Sci.* **1983**, *135*, 184.
(89) Kristyan, S.; Giber, J. *Surf. Sci.* **1989**, *224*, 476.
(90) Shalaev, V. I.; Elokhina, L. V.; Kurkin, M. I. *Phys. Met. Metallogr.* **1989**, *67*, 175 (in Russian).
(91) Weigand, P.; Hofer, W.; Varga, P. *Surf. Sci.* **1993**, *287/288*, 350.
(92) Burton, J. J.; Helms, C. R.; Polizzotti, R. S. *J. Vac. Sci. Technol.* **1976**, *13*, 204.
(93) Gates, B. C.; Katzer, J. R.; Schuit, G. C. A. *Chemistry of catalytic processes*; McGraw-Hill: New York, 1979; p 201.
(94) Toyoshima, I.; Somorjai, G. A. *Catal. Rev. Sci. Eng.* **1979**, *19*, 105.
(95) Nieuwenhuys, B. E. *Surf. Sci.* **1983**, *126*, 307.
(96) Samsonov, G. V., Ed. *The oxide handbook*; Turton, C. N., Turton, T. I., translators; Plenum: London, 1973; pp 217, 221.
(97) Chen, M.; Schmidt, L. D. *J. Catal.* **1979**, *56*, 198.
(98) Harada, M.; Asakura, K.; Ueki, Y.; Toshima, N. *J. Phys. Chem.* **1992**, *96*, 9730.
(99) Oudar, J. In *Catalyst deactivation*; Petersen, E. E., Bell, A. T., Eds.; Chemical Industries; Marcel Dekker: New York, 1987; Vol. 30, p 149.
(100) Palczewska, W. *Adv. Catal.* **1975**, *24*, 245.
(101) Paál, Z., Menon, P. G., Eds. *Hydrogen effects in catalysis, fundamentals and practical applications*; Marcel Dekker: New York, Basel, 1987.
(102) Christmann, K. *Surf. Sci. Rep.* **1988**, *9*, 1.
(103) Eberhardt, W.; Greuter, F.; Plummer, E. W. *Phys. Rev. Lett.* **1981**, *46*, 1085.
(104) Menon, P. G.; Froment, G. F. In *Metal−support and metal-additive effects in catalysis*; Imelik, B., et al., Eds.; Studies in Surf. Sci. and Catal.; Elsevier: Amsterdam, 1982; Vol. 11, p 171.
(105) Lisowski, W.; Duś, R. *Appl. Surf. Sci.* **1994**, *78*, 363.
(106) Flanagan, T. B.; Sakamoto, Y. *Platinum Met. Rev.* **1993**, *37*, 26.
(107) Caga, I. T.; Winterbottom, J. M. *J. Catal.* **1979**, *57*, 494.
(108) Cocco, G.; Carturan, G.; Enzo, S.; Schiffini, L. *J. Catal.* **1984**, *85*, 405.
(109) Szabo, A.; Paál, Z.; Szász, A.; Kojnok, J.; Fabian, D. J. *Appl. Surf. Sci.* **1989**, *40*, 77.
(110) Noh, H.; Flanagan, T. B.; Sakamoto, Y. *Script. Metallur. Mater.* **1993**, *29*, 445.
(111) Flanagan, T. B.; Noh, H. *J. Alloys Compounds* **1995**, *231*, 1.
(112) Noh, H.; Flanagan, T. B.; Sakamoto, Y. *J. Alloys Compounds* **1995**, *231*, 10.
(113) Fukai, Y.; Okuma, N. *Jpn. J. Appl. Phys.* **1993**, *32*, L1256.
(114) Oates, W. A.; Wenzl, H. *Script. Metallur. Mater.* **1994**, *30*, 851.
(115) Grill, C. M.; McLaughlin, M. L.; Stevenson, J. M.; Gonzalez, R. D. *J. Catal.* **1981**, *69*, 454.
(116) Schmidt, L. D.; Lee, C.-P. In *Catalyst deactivation*; Petersen, E. E., Bell, A. T., Eds.; Chemical Industries; Marcel Dekker: New York, 1987; Vol. 30, p 297.
(117) Boudart, M.; Wang, H. S. *J. Catal.* **1975**, *39*, 44.
(118) Chou, P.; Vannice, M. A. *J. Catal.* **1987**, *104*, 1.
(119) Bonivardi, A. L.; Baltanás, M. A. *J. Catal.* **1992**, *138*, 500.
(120) Sepúlveda, J. H.; Fígoli, N. S. *Appl. Surf. Sci.* **1993**, *68*, 257.
(121) Rousset, J. L.; Cadrot, A. M.; Cadete Santos Aires, F. J.; Renouprez, A.; Mélinon, P.; Perez, A.; Pellarin, M.; Vialle, J. L.; Broyer, M. *J. Chem. Phys.* **1995**, *102*, 8574.
(122) Rousset, J. L.; Khanra, B. C.; Cadrot, A. M.; Cadete Santos Aires, F. J.; Renouprez, A. J.; Pellarin, M. *Surf. Sci.* **1996**, *352−354*, 583.
(123) Karpiński, Z.; Kościelski, T. *J. Catal.* **1979**, *56*, 430.
(124) Guczi, L.; Karpiński, Z. *J. Catal.* **1979**, *56*, 438.
(125) Haro, J.; Gómez, R.; Ferreira, J. M. *J. Catal.* **1976**, *45*, 326.
(126) Dexpert, H.; Freund, E.; Lesage, E.; Lynch, J. P. In *Metal−support and metal-additive effects in catalysis*; Imelik, B., et al., Eds.; Studies in Surf. Sci. and Catal.; Elsevier: Amsterdam, 1982; Vol. 11, p 53.
(127) Yao, H. C.; Gandhi, H. S.; Shelef, M. In *Metal−support and metal-additive effects in catalysis*; Imelik, B., et al., Eds.; Studies in Surf. Sci. and Catal.; Elsevier: Amsterdam, 1982; Vol. 11, p 159.
(128) Huizinga, T. Ph.D. Thesis, Eindhoven University of Technology, The Netherlands, 1983.
(129) Yao, H. C. *Appl. Surf. Sci.* **1984**, *19*, 398.
(130) Anderson, A. B.; Ravimohan, C.; Mehandru, S. P. *Surf. Sci.* **1987**, *183*, 438.
(131) Juszczyk, W.; Karpiński, Z.; Ratajczykowa, I.; Stanasiuk, Z.; Zieliński, J.; Sheu, L.-L.; Sachtler, W. M. H. *J. Catal.* **1989**, *120*, 68.
(132) Muto, K.-I.; Katada, N.; Niwa, M. *Appl. Catal.* **1996**, *A134*, 203.
(133) Sprys, J. W.; Mencik, Z. *J. Catal.* **1975**, *40*, 290.
(134) den Otter, G. J.; Dautzenberg, F. M. *J. Catal.* **1978**, *53*, 116.
(135) Cairns, J. A.; Baglin, J. E. E.; Clark, G. J.; Ziegler, J. F. *J. Catal.* **1983**, *83*, 301.
(136) Kepiński, L.; Wołcyrz, M.; Jabłoński, J. M. *Appl. Catal.* **1989**, *54*, 267.
(137) Juszczyk, W.; Łomot, D.; Karpiński, Z.; Pielaszek, J. *Catal. Lett.* **1995**, *31*, 37.
(138) Venezia, A. M.; Duca, D.; Floriano, M. A.; Deganello, G.; Rossi, A. *Surf. Interface Anal.* **1992**, *19*, 543.
(139) Venezia, A. M.; Rossi, A.; Duca, D.; Martorana, A.; Deganello, G. *Appl. Catal.* **1995**, *A 125*, 113.
(140) Goetz, J.; Volpe, M. A.; Sica, A. M.; Gigola, C. E.; Touroude, R. *J. Catal.* **1995**, *153*, 86.
(141) Baker, R. T. K.; Stevenson, S. A.; Dumesic, J. A.; Raupp, G. B.; Tauster, S. J. In *Metal−support interactions in catalysis, sintering, and redispersion*; Stevenson, S. A., Baker, R. T. K., Dumesic, J. A., Ruckenstein, E., Eds.; Van Nostrand Reinhold Catalysis series: New York, 1987; p 46.